



n Ge, Zhiyu Zhu\*, Yuewei Dai\*, Biao Wang, Xuedong

School of Electronic Information, Jiangsu University of Science and Technology, Zhenjiang 212003, China

## Article info

Article history: 2021 9 17  
2021 12 22 2022  
2 1 3

Keywords: 3D

## Abstract

**Background and objective:**

가

**Methods:** , 10

가

**Discussion and results:**

(1) 가 , (1)  
(2)

**Conclusion:**

, 3D ,

© 2022 Elsevier B.V.

1. : , 가 UAV, , [1] [2] ( : , 가 ) , 가 , 가

\* Corresponding authors.

E-mail addresses: [zhuzy@just.edu.cn](mailto:zhuzy@just.edu.cn) (Z. Zhu), [dywjust@163.com](mailto:dywjust@163.com) (Y. Dai).

The diagram illustrates the historical progression of face recognition technology. It begins with the first face recognition system in 1965, followed by the use of Support Vector Machines (SVM) in 2001. A significant milestone is the AlexNet convolutional neural network in 2012, which achieved a 100% accuracy on the ILSVR dataset. Other notable models include Lenet-3 (98% accuracy), MobileNetV2 (2018), and various other models like Facenet, Wen et al., and Cosface. The timeline ends with the MobileNetV2 architecture in 2018, which achieved a 100% accuracy on the ILSVR dataset.

## 2.

### 2.1. Review of face recognition technology

Figure 1: Performance of various face recognition methods on the LFW dataset. The plot shows accuracy versus the number of training images (log scale). The methods are labeled with their names and corresponding accuracy values. The plot shows that performance generally increases with more training images, with DeepFace[9] and DeepId2[8] achieving the highest accuracy at 100,000 training images.

Method	Training Images	Accuracy
Sun	~10,000	~0.15
DeepId [5]	~10,000	~0.25
Zhu	~10,000	~0.20
DeepId	~10,000	~0.25
LFW	~10,000	~0.25
DeepId2 [6]	~10,000	~0.25
DeepId2	~10,000	~0.25
DeepId2 + [7]	~10,000	~0.25
DeepFace[9], DeepId2[8]	100,000	~0.45

## 2.2. Research status of target detection at home and abroad

```

graph TD
    Input[Input Image] --> RCNN16[R-CNN [16]]
    RCNN16 --> SVM[SVM]
    SVM --> FRCNN19[Fast R-CNN [19]]
    FRCNN19 --> RPN1[RPN]
    RPN1 --> FRCNN20[Fast R-CNN [20]]
    FRCNN20 --> RPN2[RPN]
    RPN2 --> RFCN30[R-FCN [30]]
    RFCN30 --> ROI[ROI]
    ROI --> PSROI[PSROI]
    PSROI --> RFCN31[R-FCN [31]]
    RFCN31 --> YOLOv233[YOLOv2 [33]]
    YOLOv233 --> YOLOv233
  
```

The diagram illustrates the architecture of the proposed YOLOv2 model. The process starts with an input image, which is processed by a convolutional layer (R-CNN [16]) and then a support vector machine (SVM). This is followed by a Fast R-CNN [19] block, which includes a region proposal network (RPN). The output of the RPN is then processed by a Fast R-CNN [20] block, which also includes an RPN. The final output is a set of bounding boxes (R-FCN [30]) and a region of interest (ROI). The ROI is then processed by a region of interest pooling (PSROI) block, which outputs a set of bounding boxes (R-FCN [31]). The final output is a set of bounding boxes (YOLOv2 [33]). The diagram also shows the relationship between the proposed YOLOv2 model and the YOLOv2 model, indicating that the proposed model is a modified version of the YOLOv2 model.

The diagram illustrates the relationships between various deep learning models and their components. The central part of the diagram is labeled "3.2. Joint optimization method".

**Models and Components:**

- YOLOv3 [21]:** darknet-53, YOLOv3 FPN [ [34] ]
- SSD [ [35] ]:** SSD, SSD (Single Shot MultiBox Defender), Yolo (You Only Look Once)
- R-CNN, Fast R-CNN, Fast R-CNN:** R-CNN(Region-CNN), R-CNN, FastR-CNN, Fast R-CNN
- AlexNet-Emotion:** AlexNet-Emotion
- Softmax:** Softmax
- Island:** Island

**Connections:**

- YOLOv3 [21] is connected to darknet-53 and YOLOv3 FPN [ [34] ].
- SSD [ [35] ] is connected to SSD, SSD (Single Shot MultiBox Defender), and Yolo (You Only Look Once).
- R-CNN, Fast R-CNN, and Fast R-CNN are connected to R-CNN(Region-CNN), R-CNN, FastR-CNN, and Fast R-CNN.
- AlexNet-Emotion is connected to AlexNet-Emotion.
- Softmax is connected to Softmax.
- Island is connected to Island.

**3.2. Joint optimization method**

The diagram shows a complex network of relationships between these models and components, with arrows indicating the flow of information or the direction of the relationships. The central part of the diagram is labeled "3.2. Joint optimization method".

3.

### 3.1. Depth target detection algorithm

Figure 1: Comparison of the proposed PU (Deep OD) and GAN-based methods. The figure shows two rows of images. The top row is labeled 'PU (Deep OD)' and the bottom row is labeled 'GAN-based methods'. Each row contains four images of a person's face. The first image in each row is a reference image. The second image in the 'PU (Deep OD)' row is labeled '가' and the second image in the 'GAN-based methods' row is labeled '가'. The third image in the 'PU (Deep OD)' row is labeled '가' and the third image in the 'GAN-based methods' row is labeled '가'. The fourth image in the 'PU (Deep OD)' row is labeled '가' and the fourth image in the 'GAN-based methods' row is labeled '가'. The 'PU (Deep OD)' row shows more realistic and diverse results compared to the 'GAN-based methods' row.

$$L_c = \frac{1}{2} \sum_{i=1}^m \max (||x_i - c_{y_i}||^2 - \tau, 0) \quad (1)$$

가 . Island Loss

$$L_{LL} = L_c + \frac{1}{2} \sum_{c_j \in K} \sum_{c_k \in K, c_k \neq c_j} \left( \frac{c_k c_j}{\|c_k\|_2 \|c_j\|_2} + 1 \right) \quad (2)$$

Emotion

$$L = L_s + L_{LL} \quad (3)$$

$$L_s = -\frac{1}{m} \sum_{i=1}^m \log \frac{e^{z_{yi}}}{\sum_{j=1}^m e^{z_{yj}}} = -\frac{1}{m} \sum_{i=1}^m \log \left( \frac{e^{w_{yi}^T x_i + b_{y_i}}}{\sum_{j=1}^m e^{w_{yj}^T x_i + b_{y_j}}} \right) \quad (4)$$

Island

$$\Delta c_j = \frac{\sum_{i=1}^m \delta(y_i, j) (c_j - x_i)}{1 + \sum_{i=1}^m \delta(y_i, j)} + \frac{\lambda_1}{|K| - 1} \sum_{\substack{c_k \in N \\ c_k \neq c_j}} \frac{c_k}{\|c_k\|_2 \|c_k\|_2} - \left( \frac{c_k \cdot c_j}{\|c_k\|_2 \|c_j\|_2} \right) c_j \quad (5)$$

$$c_j^{t+1} = c_j^t - a c_j^t \quad (6)$$

$$= j, \delta(y_i, j) = 1; y_i \neq j, \delta(y_i, j) = 0$$

IRNN

motion

4.1

가

$$a_i = c^T V h_i \quad (7)$$

$$i = \frac{\exp(a_i)}{\sum_{t=1}^T a_t} \quad (8)$$

$$f_v = \sum_{l=1}^T \xi_l h_l \quad (9)$$

IRNN

### 3.3. Occluded face recognition model based on dual discrimination countermeasure network

가

4.

#### 4.1. Deep facial expression recognition based on static image

가

가

AlexNet(Krizhevsky et al., 2012), visual geometry group(VGG, [27]), VGG-Face(Parkhi et al., 2015) GoogLeNet [37]

CFW(cellular face in the wild)(Zhang, 2012) F aceScrub (Ng Winkler, 2014)

FER2013(Goodfellow, 2013) TFD(Toronto to face

Kaya (2017) VGG

Imagenet [28]

가

FE R 2013 (EmotiW)

Face et2ExpNet

Ding et al. (2

가

가

가

#### 4.2. Deep facial expression recognition network based on dynamic image sequence

가

가

가

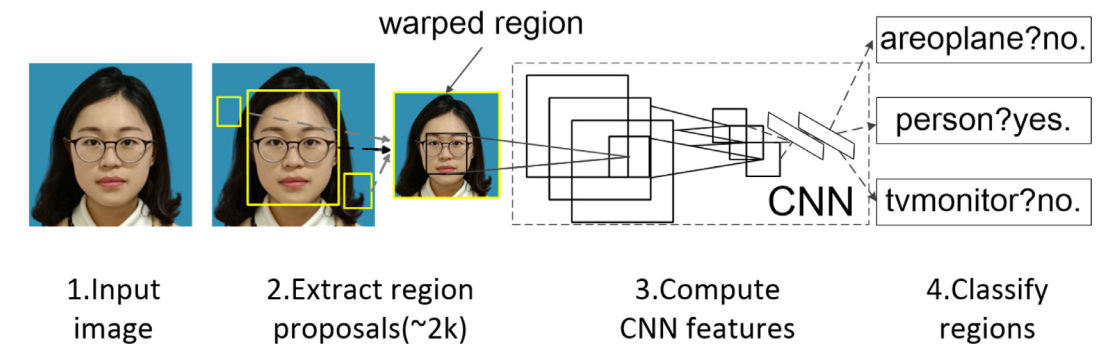


Fig. 1. Architecture of R-CNN.

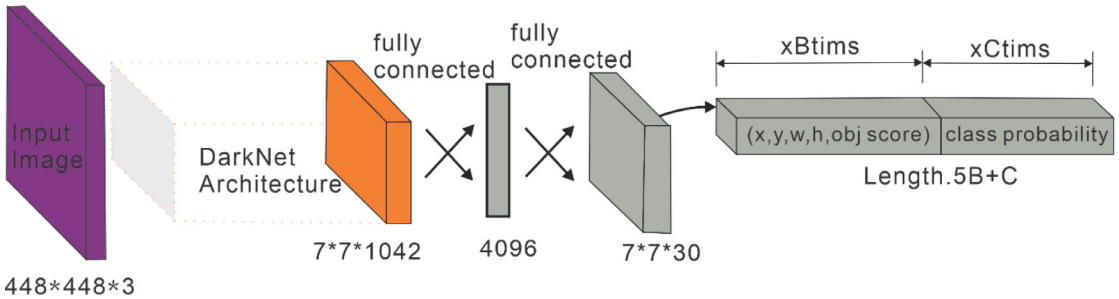
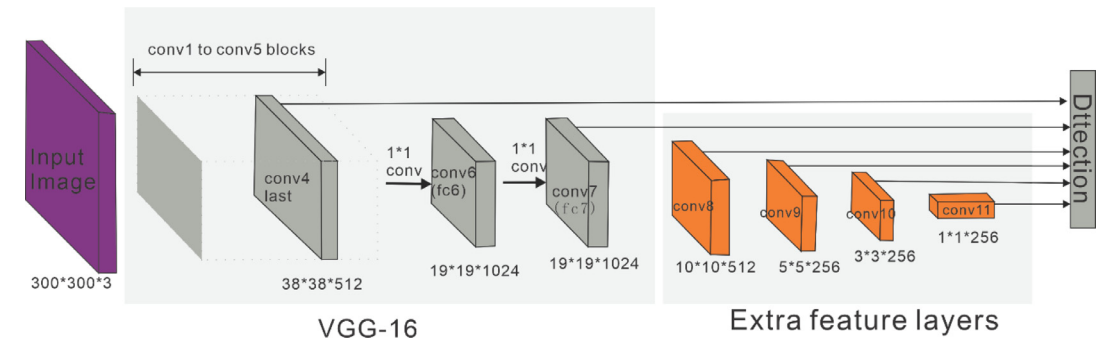


Fig. 2. Architecture of YOLO.



3. SSD

4.3. Summary of target detection based on deep learning

2

. 2

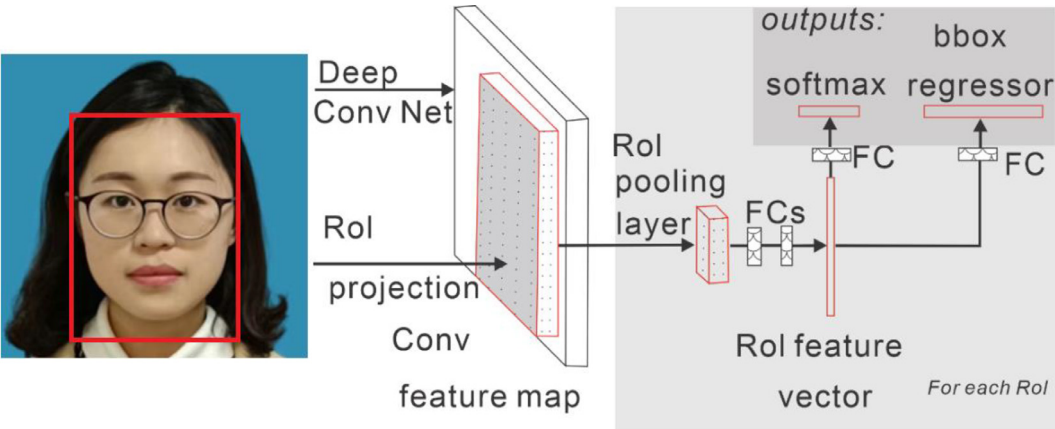
RNN

CNN-RNN

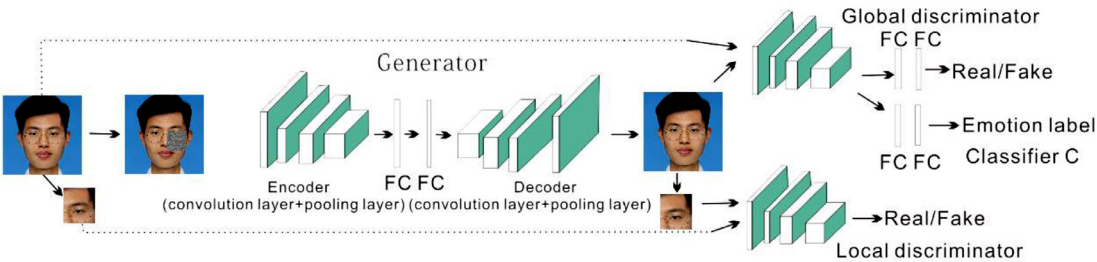
[24].

AlexNet-Emotion

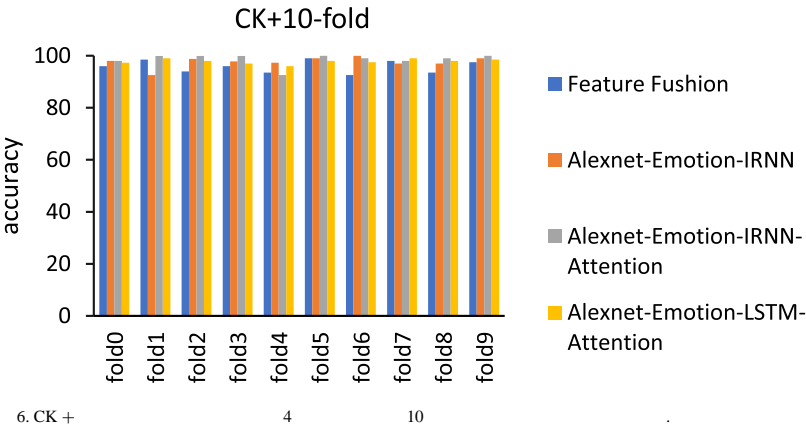
AlexNet-Emotion



4. Fast R-CNN



5.



1

(MAP)

Algorithm	CK+	MMI
AUDN	93.7%	75.85%
DeRL	96.57%	72.67%
IL-CNN	94.39%	70.67%
Inception	93.2%	77.6%
IACNN	95.37%	71.55%
AlexNet-Emotion linit	94.41%	65.88%
AlexNet-Emotion Softmax loss	96.45%	76.89%
AlexNet-Emotion w/o Angle Variance	93.73%	71.84%
AlexNet-Emotion Pre	97.14%	78.68%

DeR L(deexpression residual learning)

Island loss optimization [25]

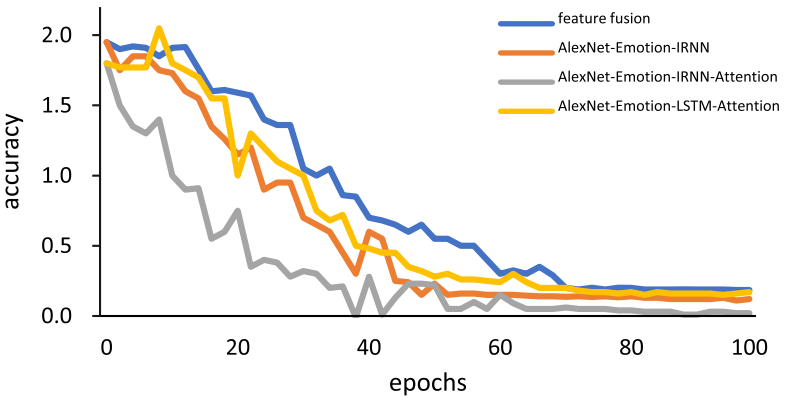
Mollahoseini

AlexNet-Em

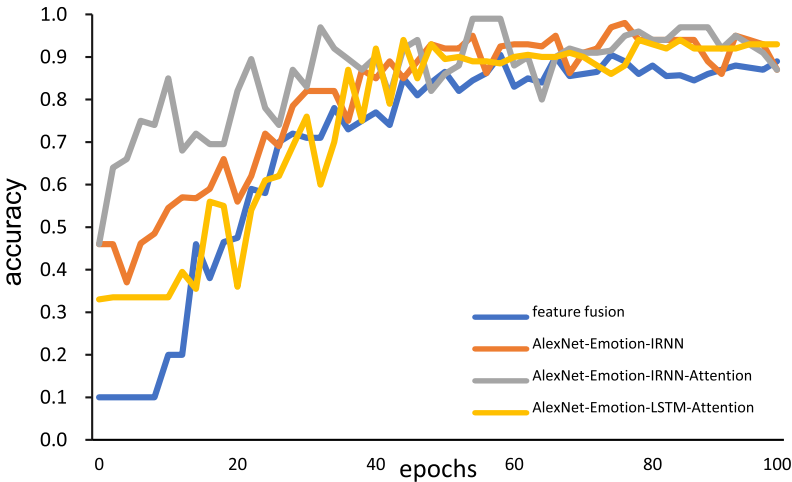
otion

1

[26]



(a)

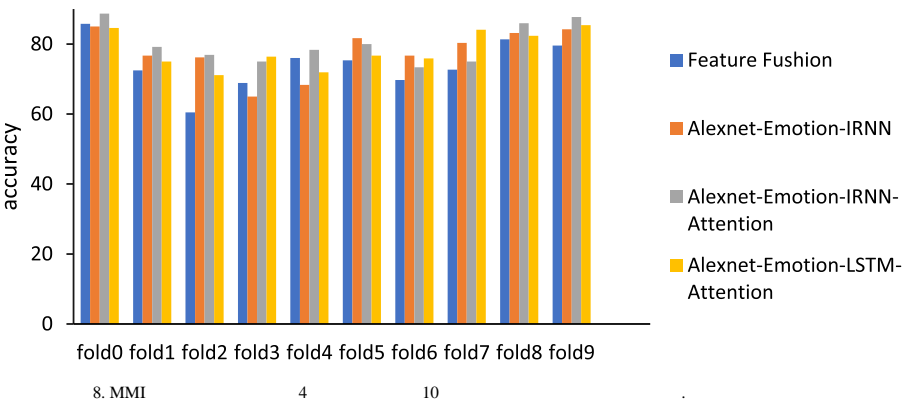


(b)

7. (a) 4

(b)

MMI 10-fold



8. MMI

4

10

AlexNet-Emotion

5.

CK +  
( 6)가  
4  
( 8).

4  
( 7).  
10

, MMI  
가

가  
가

egories( ).

가

가

가

, 3D

6.

가

가

가

( 1-3, (1)-(9)).

[5] Y. Sun, X. Wang, X. Tang, 10,000, IEEE, 2014, pp. 1891–1898. [6] Y. Sun, Y. Chen, X. Wang, 2014, pp. 1988–1996. [7] Y. Sun, X. Wang, X. Tang, IEEE, 2015, pp. 2892–2900. [8] F. Schroff, D. Kalenichenko, J. Philbin, Facenet: A deep learning framework for face verification, IEEE, 2015, pp. 815–823. [9] Y. Taigman, M. Yang, M.A. Ranzato, et al., Deepface: Face verification in the wild, IEEE, 2014, pp. 1701–1708. [10] Y. Wen, K. Zhang, Z. Li, et al., Deep learning of face representations for face verification, Springer, Cham, 2016, pp. 499–515. [11] W. Liu, Y. Wen, Z. Yu, et al., Deep learning of face representations for face verification, 2, ICML, 2016, p. 7. [12] F. Wang, J. Cheng, W. Liu, 가, IEEE Signal Processing Letters, 25, PISCATAWAY, USA, 2018, pp. 926–930. [13] H. Wang, Y. Wang, Z. Zhou, CosFace: A deep learning framework for face verification, IEEE, 2018, pp. 5265–5274. [14] S. Chen, Y. Liu, X. Gao, MobileFaceNets: A deep learning framework for face verification, Springer, Cham, Berlin, 2018, pp. 428–438. [15] M. Sandler, A. Howard, M. Zhu, et al., MobileNetV2: A deep learning framework for face verification, IEEE, 2018, pp. 4510–4520. [16] R. Girshick, J. Donahue, T. Darrell, et al., Faster R-CNN, IEEE, 2014. [17] Zhu G., Porikli F., Li H. A. Van De Sande, T. Gevers, et al., Int. J. Comput. Vis. 104(2) (2013) 154–171. [19] C. Lee, J.H. Kim, K.W. Oh, R-CNN [C]//2016 16 (iccas), IEEE, 2016, pp. 107–110. [20] S. Ren, K. He, R. Girshick, Faster R-CNN: A deep learning framework for face verification, IEEE, 39(6)(2016) 1137–1149. [21] X.X. Zhang, X. Zhu, YOLOv3, Int. J. Remote Sens. 41(11)(2020) 4312–4335. [22] Nguyen H.T., Université de Grenoble, 2014. [23] Z. Tang, G. Zhao, T. Ouyang, Renew. Energy 173 (2021) 1005–1016, doi: 10.1016/j.renene.2021.04.041. [24] C. Lunerti, R.M. Guest, R. Blanco-Gonzalo, et al., IEEE 51st International Carnahan Conference on Security Technology, IEEE, 2017. [25] Z.H. Tang, Y.Y. Li, X.Y. Chai, H.Y. Zhang, S.X. Cao, NOx, J. Chem. Eng. Jpn. 53 (1) (2020) 36–44, doi: 10.1252/jcej.19we142. [26] L.C. Yan, B. Yoshua, H. Geoffrey, Nature 521 (7553) (2015) 436–444. [27] Simonyan K., Zisserman A., arXiv:1409.1556, 2014. [28] Knyazev B., Shvetsov R., Efremova N., et al. arXiv:1711.04598, 2017. [29] Yue-Hei Ng J, Hausknecht M, Vijayanarasimhan S, et al. : [C]//IEEE, 2015: 4694-4702. [30] Gabrielsson S.

[1] C. He, Intell.Comput.Appl. 6(5)(2016) 112–114. [2] M.H. Zhu, S.T. Li, Y. Hua, Pattern Recognit.Artif.Intell. 27(8)(2014) 708–712. [3] Y.L. Xue, X. Mao, C. Catalin-Daniel, J. Beijing Univ. Aeronaut. Astronaut. 36(4)(2010) 429–433. [4] Y. Chenglin, P. Hailong, Comput.Electr.Eng. 92(2021) 92.



[32] W. Chen, M. Fang, Y.H. Liu, et al., in: SLAM[C]/2017, IEEE, 2017, 599-604. [33] Xu X., Dou P., Le H.A., et al. 3D 2D UR2D[J]. arXiv:1709.06532, 2017. [34] J. Wang, J. Ding, H. Guo, et al., OBB: 11(24)(2019) 2930. [35] Felsberg M., 5 : [J]. 2017. [36] Rezaei M, Azarmi M. Deepsocial: 19 7[J]. , 2020, 10(21): 7514. [37] S. Paul, L. Singh, C//2015 IEEE : , (WCI), IEEE(2015) 1 – 6. [38] H Ge, Y Dai, Z Zhu, et al., [J], 11(24)(2021) 11588.